Evaluation of Point of Load Converters for Space Computational Loads

Thomas Cook, Aidan Phillips, Christopher Siak, Alan D. George, and Brandon M. Grainger
NSF Center for Space, High-Performance, and Resilient Computing (SHREC)
University of Pittsburgh
3700 O'Hara St.
Pittsburgh, PA 15261
{tvc8 / amp318 / cjs188 / alan.george / bmg10}@pitt.edu

***Abstract*—Space experiments in low earth orbit (LEO) are becoming more ambitious and the power electronic systems for these missions are quickly becoming outdated when compared to the power-dense and highly efficient commercial solutions used to power modern processors. In this work, a comparison is presented between several radiation-hardened (rad-hard) and commercial-off-the-shelf (COTS) point-of-load (PoL) converters with a focus on Gallium Nitride (GaN) switching FETS. The converters were designed and evaluated based on their electrical and thermal performance when supplying power to computational loads in a LEO environment. This work is presented in the context of supplying power to a 1U FPGA-based computing platform that features a mix of COTS and rad-hard components, and a modular power system.**

TABLE OF CONTENTS

1. INTRODUCTION

With the increased number of commercial satellite launches in the past decade, the need for small, capable, and inexpensive processing systems has widened. Many in the space community are considering the move from multi-million-dollar projects to smaller, more replaceable satellites to accomplish their science objectives [1]. The space industry is set to expand to over $8.8 billion dollars by 2030 fueled by the rapid increase in the number of small satellite launches and decreased costs resulting from rideshare companies and programs [1, 2]. Many research and science experiments are currently on the International Space Station (ISS), which allows access to LEO space with a reliable bus for communication and power [3, 4]. With these more complex and ambitious experiments launching into orbit, a need exists for high-efficiency, compact, and inexpensive converters to power these missions. Converter power losses create significant heat and large package sizes waste valuable space that could be used for additional computational or remote sensing capabilities. These problems often require complex thermal and structural design tradeoffs that increase mission complexity and cost.

The motivation of this paper is the development of a power system for use on a new 1U-sized (10cm x 10cm) FPGA-based computing platform called the SHREC Space Processor (SSP), and looks specifically at several PoL power electronic converters used to generate the 1.0V, 1.8V. and 3.3V voltages that are common for use in computational loads. A COTS Linear Technologies LTC7151S, two rad-hard converters the Texas Instruments TPS50601A-SP and Renesas ISL70001ASEH, and three experimental GaN converters based on the Linear Technologies LTC3833 controller are all evaluated and compared for electrical and thermal performance. The potential benefits of GaN are also discussed for its power electronic and radiation performance that makes it very useful for small spacecraft. Finally, in-situ electrical performance measurements are presented of several GaN converters flying on the ISS.

2. MOTIVATION

The following section provides an overview of the design and layout of the power system for an FPGA-based computing platform as well as the design of drop-on converter modules.

SHREC Space Processor (SSP)

The CHREC Space Processor (CSP) is an inexpensive but highly reliable 1U-sized hybrid reconfigurable computing platform featuring a mix of COTS and rad-hard components augmented by fault-tolerant computing techniques developed by researchers at the NSF SHREC Center. The newest revision of this technology, the SSP, which builds upon the CSP, has four times more FPGA resources while maintaining the 1U form factor and is shown in Figure 1. The original CSP used approximately 3.5W of power while the SSP can use up to 14W, due in part to the incorporation of multi-gigabit transceivers (MGTs) and a powerful Xilinx Zynq 7045 SoC. The increase in power required the use of a new

978-1-7821-2734-7/20/$31.00 ©2020 IEEE

power system architecture and different converters that were small yet powerful enough to meet increased demand. The SSP has up to 16GB of DDR3L RAM and 64GB of NAND flash for computational resources. A rad-hard watchdog monitors the heartbeat of the Zynq and power converters that can reset the Zynq in the event of a single-event latch up (SEL). The first use of the SSP will be on the Department of Defense Space Test Program Houston 7 Mission (STP-H7) to the ISS with the CASPR experiment and will be used as an image capture and processing device for several novel sensors. The CSP will act as a controller for the experiment due to its flight-proven design.

SSP Power System Layout

The SSP is powered from 5V and 3.3V voltage rails from 8 pins (14.4A) and 4 pins (7.2A) respectively of a SAMTEC 244 pin connector. A total of three switching converters are powered from the 5V rail and four low drop-out regulators (LDOs) powered from the 3.3V rail make up the power system of the SSP. All converters were designed to meet the operating criteria for the Zynq 7045 which has the capability to use over 20W of power with a base power draw of approximately 4W. Converter output ripple was to be minimized to 20mV, with load transient over and under-voltage response being designed to the strictest datasheet requirement of +/-30mV for the 1.0V VCCPINT rail. The startup sequence of all converters and LDOs was designed according to the datasheet for each critical bank voltage. The 1.0V rail converter has the capability to draw approximately 10A with a maximum voltage overshoot of 30mV. Dual TI

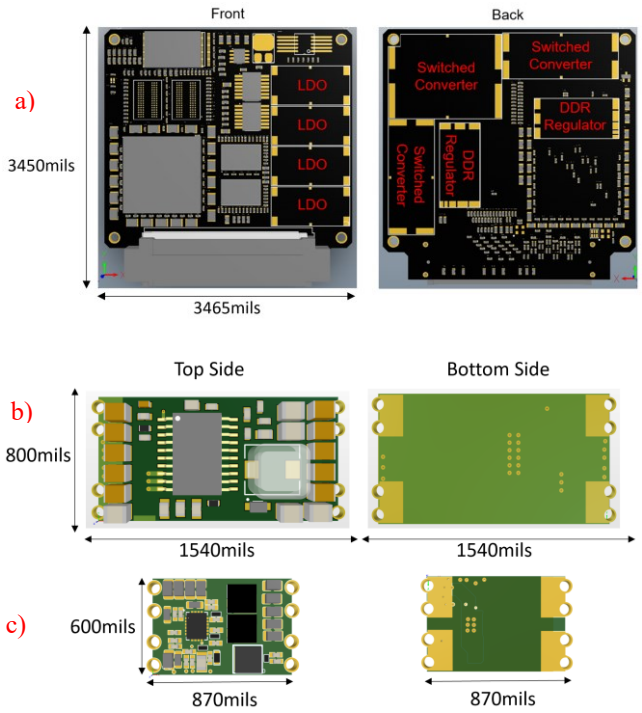

Figure 1. a) SSP Layout with experimental converter module placement. b) Experimental converter module layout and underside pad layout for the TPS50601A-SP, and c) LTC3833 with GaN Systems GS61004B HEMTs

TPS50601A-SP 6A converters are used to supply the 1.0V rail. The 1.8V and 1.35V use single TI TPS50601A-SP converters and each of the rails are only expected to draw approximately 2.5A with a maximum overshoot of 90mV.

The SSP provides the framework for MGT protocols like SRIO and Aurora which are very high bandwidth communication and data-transfer interfaces. TI TPS7H1101-SP LDOs are used due to the tight voltage regulation requirements of 10mV for the protocols. MGTs require up to 1.9A of drive current and when powered off of 3.3V supplied LDOs makes for a system with significant power loss.

Additionally, the SSP has four DDR3L modules, one NAND flash module, power sequencing circuitry, and a watchdog circuit. The DDR3L is arranged in two banks for the processing system (PS) and programmable logic (PL) sides of the Zynq SoC. Both DDR banks are powered from a 1.35V TI TPS7H3301-SP DDR regulator that produces the 0.675V reference voltage and can simultaneously sink or source up to 3A. Power sequencing is accomplished by cascading each converter's and LDO's "power good" and "enable" signals with an RC time constant to power up the Zynq in the correct order. The watchdog works in conjunction with the power sequencing that in the event of an upset or latch up, the watchdog will power-cycle the Zynq forcing a restart.

Modular Power System Architecture

The CSP utilized a "selective population" parts scheme in order to employ both COTS and rad-hard components on the same PCB. This layout, while cost-efficient, wasted approximately 30% of the board space of the CSP. The SSP comes in two different versions, a full COTS solution and a hybrid solution featuring a mix of rad-hard and COTs components. An experimental version of the SSP is planned to use drop-on modules for all switched converters and LDOs that allows for COTS or rad-hard parts to be exchanged easily. If a converter goes bad or a part becomes unavailable, only the converter itself needs to be replaced and the whole board does not need reassembly. Only the input and output characteristics of the replacement module need to be matched. The drop-on module provides flexibility for converter manufacture selection as well as allowing for the potential use of more experimental GaN converters. Each module has connections for V_{in} and V_{out}, with individual GND connections as well as enable and power good signals used for power sequencing. Castellated vias and bottom-side pads are used for making the electrical connections, and non-conductive epoxy is used to increase the mechanical stability of the module. This style of module connection was successfully flown on the Spacecraft Supercomputing for Image and Video Processing (SSIVP) experiment as part of the Department of Defense Space Test Program Houston 6 Mission (STP-H6) to the ISS in 2019 [3].

3. GaN Technology

While the space power electronics industry has primarily been dominated by silicon technologies, radiation testing of

GaN has shown positive radiation performance while simultaneously offering better switching performance compared to silicon [5, 6]. GaN devices provide comparable or higher efficiencies with lower volumes, mass, and cost when compared to conventional silicon rad-hard converters. The GaN high electron mobility transistors (HEMTs), which are a type of heterojunction field-effect transistor, tested in this paper are shown in Table 1 [7-9].

Table 1. GaN HEMT Parameters

Parameter	EPC2014C	EPC2015C	GS61004B
Drain-Source Voltage	4.5 – 40 V	4.5 – 40 V	3.8 – 100 V
Continuous Drain Current	10A	53A	45A
Threshold Gate-Source Voltage	1.4 V	1.4V	1.6 V
Maximum Gate-Source Voltage	6 V	6V	7 V
Minimum Gate-Source Voltage	-4V	-4V	-10V
On Resistance	16 mΩ	4 mΩ	15 mΩ
Gate Charge	2.5 nC	8.7 nC	6.6 nC
Package Type	Passivated BGA Die	Passivated BGA Die	GaN_{px}

Power Semiconductor Device Performance

GaN HEMTs allow electrons to move freely in the device as a 2D "gas" and which provides a fast gate turn-on [6, 10, 11]. In power electronic devices, GaN HEMTs offer several advantages over silicon, primarily with a significantly wider band-gap of 3.4eV compared to the 1.12eV gap of silicon [10]. The large band-gap energy allows GaN devices to operate at a higher temperature, despite poorer thermal conductivity [12]. Manufacturers have been able to improve GaN thermal conductivity with advanced packaging techniques, and have been able to achieve similar performance levels as silicon [13, 14]. The larger energy gap also allows the physical depletion region of the transistor to shrink while maintaining a high blocking and breakdown voltage. The smaller depletion region has the added benefit of reducing ON resistance that improves the efficiency of switching converters during conduction.

The small gate capacitance of GaN HEMTs allow switching at much higher frequencies with lower losses than silicon, making them very popular for radio frequency (RF) amplifier applications [11]. GaN HEMTs have no body diode due to manufacturing, eliminating diode reverse recovery loss during switching, further improving efficiency [15]. With the combination of low gate capacitance and high-voltage switching capabilities, GaN allows designers to increase switching frequency that reduces magnetic device sizing and maintain the same output power of a silicon-based converter. GaN transistors are approximately 1/10th the size of a comparable silicon MOSFET, and providing the same or better performance in terms of voltage rating, current rating, and ON resistance [16]. The smaller package also decreases package inductances and ringing observed during switching that allows for increased stability margins. The ability to decrease the size and weight of a converter while maintaining power output makes them an attractive option for space.

Radiation Performance

The construction and material properties of GaN HEMTs provide several advantages over silicon when operating in harsh radiation environments without the need for special manufacturing or design techniques [17, 18]. Four main types of semiconductor radiation effects can impact the performance of a transistor: total ionizing dose (TID), single event effects (SEEs), dose-rate radiation, and radiation displacement damage [6]. Throughout the duration of a mission, TID develops from high-energy particles or photons passing through the oxide layer on a transistor that eventually leads to an accumulation of charge build-up at both the gate and field oxide. The charge build-up causes the device to activate without a gate drive signal being applied. GaN HEMTs are manufactured with a Schottky metal gate that eliminates most TID effects by allowing the charge build-up to dissipate [5]. Expected TID performance of GaN is above 100krad [19]. SEE effects are mitigated by the wide bandgap of GaN HEMTs due to the much higher energy that is required for energetic ions to deposit in the material of the semiconductor to form the electron-hole pairs that induce SEEs. Expected SEE performance of GaN is above 75 MeV-cm^2/mg [19]. The smaller depletion region volumes of GaN HEMTs collect less charge, reducing the probability of dose rate radiation effects. Radiation displacement damage caused by high energy protons displacing semiconductor atoms in the semiconductors crystalline lattice has shown to very rarely impact the functionality of GaN HEMTs [5]. GaN HEMT devices have shown sensitivity to neutron radiation displacement damage that causes an increase in ON resistance and bias current while decreasing the sustained blocking voltage [6, 20]. When selecting GaN HEMTs for power electronic applications, the devices should be appropriately de-rated to account for the decrease in performance resulting from radiation effects over the lifetime of the mission. Testing at the NASA Jet Propulsion Laboratory (JPL) has shown that GaN HEMTs are extremely resistant to both radiation-induced TID and SEEs. However, more significant testing is necessary if GaN HEMTs are going to be used in a LEO, such as for the SSP [21].

4. Converter Comparison

The GaN HEMTs in Table 1 are paired with the Linear Technologies LTC3833 synchronous buck controller and are then compared to a silicon COTS Linear Technologies LTC7151S converter and two rad-hard buck converters, the Renesas ISL70001ASEH and Texas Instruments TPS50601A-SP. These converters are all excellent examples of the current market offering [22-24]. All major parameters of the converters under test are listed in Table 2.

COTS Converters

The Linear Technologies LTC7151S was selected as a representative COTS converter for incorporating several

Table 2. Converters Test Parameters

Parameters	Converters					
	TI TPS50601A-SP	Renesas ISL70001SEH	LT LTC7151S	LT LTC3833 with GaN Systems GS61004B HEMT	LT LTC3833 with EPC 2014c HEMT	LT LTC3833 with EPC 2015c HEMT
Input Voltage Range	3V to 7V	3V to 5.5V	3.1V to 20V	4.5V to 38V	4.5V to 38V	4.5V to 38V
Output Voltage	1V, 1.8V, 3.3V	1V, 1.8V, 3.3V	1V, 1.8V, 3.3V	1V, 1.8V, 3.3V	1V, 1.8V, 3.3V	1V, 1.8V, 3.3V
Maximum Output Current	6A	6A	15A	20A	10A	20A
Switching Frequency	500kHz	1MHz	500kHz	2MHz	2MHz	2MHz
Inductor	3.3µH	1µH	0.25µH	0.33µH	0.33µH	0.33µH
Input Capacitance	141uF	101uF	121uF	103.3uF	103.3uF	103.3uF
Output Capacitance	494uF	470uF	530uF	140uF	140uF	140uF
Compensation Network	6.81kΩ / 100p / 6800p	Internal	10 kΩ / 22 pF / 1 nF	16.5 kΩ / 100 pF / 670 pF	16.5 kΩ / 100 pF / 670 pF	16.5 kΩ / 100 pF / 670 pF
Thermal Operating Range	-55°C to 125°C	-55°C to 125°C	-40°C to 125°C	-40°C to 125°C	-40°C to 125°C	-40°C to 125°C
Radiation Tolerance	100krad, 75MeV	100krad, 86.5MeV	N/A	Potentially Suitable for LEO	Potentially Suitable for LEO	Potentially Suitable for LEO
FET Technology	Si, Internal	Si, Internal	Si, Internal	GaN, External	GaN, External	GaN, External
Package Size	10mm x 13mm	14.5mm x 14.5mm	4mm x 5mm	3.5mm x 4.5mm	3.5mm x 4.5mm	3.5mm x 4.5mm
FET Dimensions				4.6mm x 4.4mm	1.1mm x 1.7mm	4.1mm x 1.6mm
Watt/mm^2	0.115	0.094	0.75	0.267	0.770	0.672

Datasheet Value
DUT Operation Value

features that modern power converters have such as soft start, low EMI emissions, and monolithic integrated MOSFETs. The LTC7151S is capable of operating with a 400kHz to 3MHz switching frequency and delivers up to 15A at high-efficiency thanks to the integrated capacitors of the Silent Switcher 2 architecture. Datasheet and LT PowerCAD values were used to develop the simulation model and a 0.25µH inductor was selected with a switching frequency of 500kHz.

Rad-Hard Converters

The Texas Instruments TPS50601A-SP and the Renesas ISL70001ASEH both feature soft start, power good and enable signaling, monolithic integrated MOSFETs, and hermetic/ceramic packaging. Both converters are rated for 100krad of TID and 75MeV-cm^2/mg and 86.4MeV-cm^2/mg SEL for the TPS50601A-SP and ISL70001ASEH converters, respectively.

The TPS50601A-SP uses cycle-by-cycle current limiting on the high-side FET combined with low-side FET sourcing current limiting to protect the converter during overload and current runaway situations. The controller incorporates input and output voltage regulation with power good monitoring for protecting the device and load during voltage transients. Over-temperature is monitored and the converter will automatically turn OFF and soft start turn ON when the temperature is 10°C below the thermal trip point. The TPS50601A can be synced with another device to double the current output of the converters to 12A. The TI converter was designed with a 3.3 µH inductor with a 500 kHz switching frequency.

The ISL70001ASEH has input under-voltage, output under-voltage, and output overcurrent protection to protect the

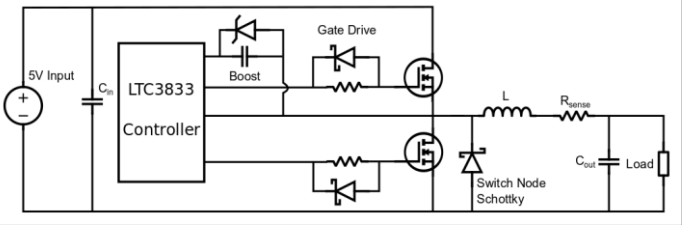

Figure 2. LT LTC3833 GaN Converter Schematic

device and load. The converter can be synchronized with other devices 180 degrees out of phase to lessen source RMS current ripple, improving efficiency and reduce EMI. The Renesas converter was designed with a 1µH inductor with a 1MHz switching frequency.

GaN Converters

The Linear Technologies LTC3833 synchronous buck controller, shown in Figure 2, can operate on a very wide voltage range up to 38V with a fast load transient response and up to 2MHz switching frequency [25]. The LTC3833 has fixed dead-time logic to safeguard the top and bottom gates from turning ON simultaneously, eliminating shoot-through and damage to the HEMTs. The controller features soft start or output voltage tracking and provides output overvoltage protection, programmable current limit with foldback, power good and enable signaling for power sequencing. Discontinuous conduction mode or pulse-skipping mode is allowable if the load current is less than half of the peak to peak inductor current ripple, which is a variable frequency mode. The LTC3833 senses inductor current with either a sense resistor or an RC circuit across the inductor (DCR sensing). The sense resistor is a more accurate measurement and is used for all GaN converters in this paper, but DCR is

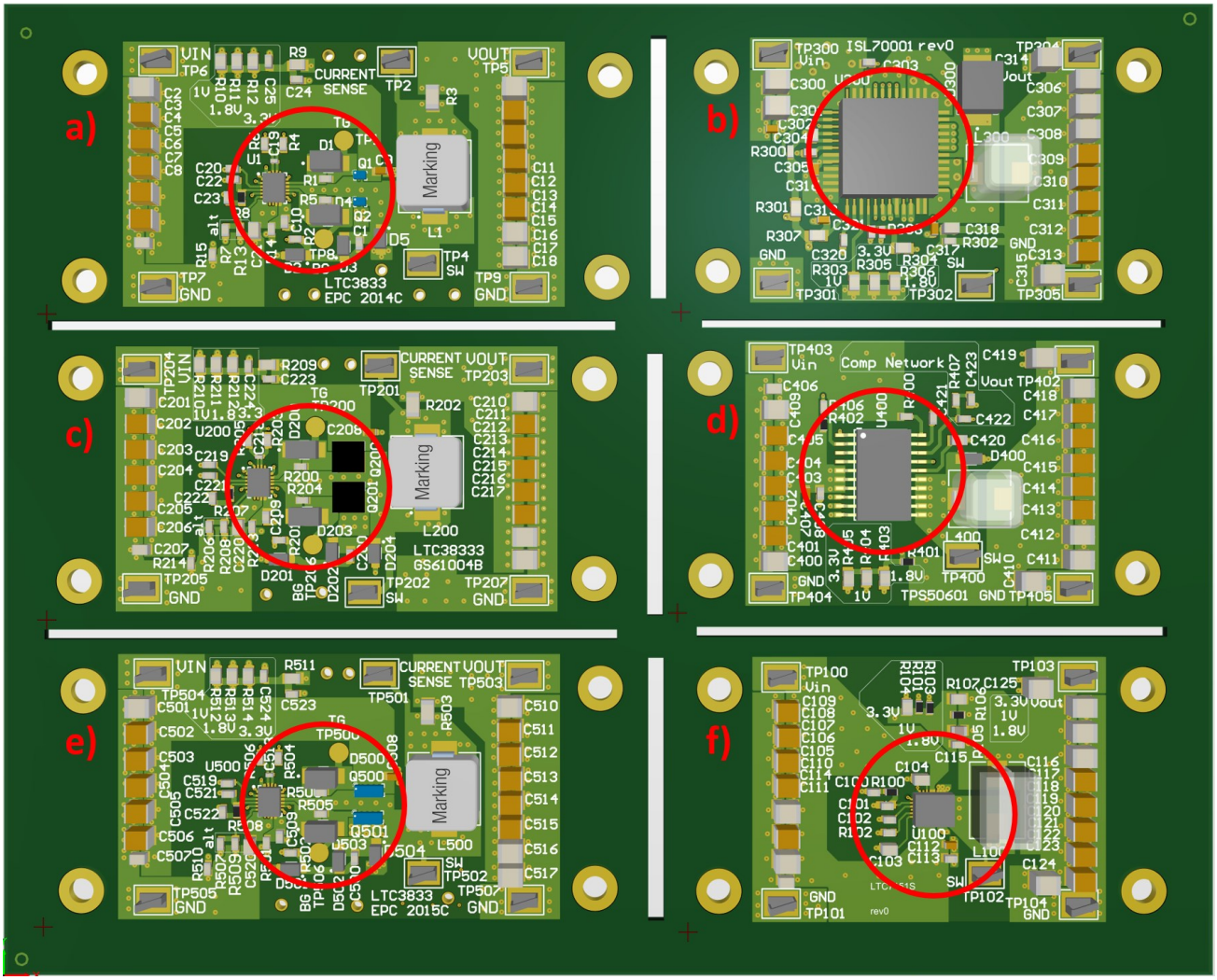

Figure 3. PCB Panel with converters under test: A) LTC3833 EPC2014C, B) ISL70001ASEH (Rad-hard), C) LTC3833 GaN Systems GS61004B, D) TI TPS50601A (Rad-hard), E) LTC3833 EPC2015C, F) LTC7151S (COTS). The red circle is a 1in diameter for scale.

more energy-efficient and saves on large high-power sense resistors. The overall converter design and GaN devices selected for this paper are similar to those that were used in the SSIVP experiment on the STP-H6 mission [3, 25]. The EPC2014C is the same part as that used on SSIVP and the GaN Systems GS61004B is functionally similar to the Teledyne TDG100E15BSDX. The EPC2015C was selected for use due to its higher current carrying capabilities and lower on-resistance over the EPC2014C while still being in the 40V rated category. Both EPC GaN HEMTs have a maximum gate drive voltage of 6V while the GaN Systems HEMT has a maximum of 7V. Testing at NASA JPL has shown the 40V rated EPC GaN HEMTs perform very well during radiation testing [21].

A key challenge of driving GaN HEMTs is controlling the gate-source voltage overshoot during device turn-on. To prevent this overshoot, a gate drive resistor was added to slightly slow the rise-time and a parallel Schottky diode was used to reduce its magnitude. The Schottky diode provides a discharge path during device turn OFF, reducing switching losses and minimizing Miller turn-on effects. A 5.1V clamping Zener diode was added across the boost capacitor to ensure the high-side drive voltage does not drift during system transients. A 40V protection Schottky diode was added at the switching node to prevent over-voltage of the GaN HEMTs. An example schematic of all GaN converters is shown in Figure 2.

5. Converter Design

The following section covers the design and PCB layout of the converters under test as well as the test equipment used for conducting the various measurements of each converter.

Board Design

PCBs were designed for experimental usage and to take measurements as shown in Figure 3, but similar designs for processor applications were also developed. The primary differences between the layouts include the removal of several test points and electrical contacts that reduced the total area by 40%.

The experimental boards have an average size of 2.5” x 2” using a four-layer stack-up of (Top) signal/power, (Layer 1) ground, (Layer 2) signal/power, (Bottom) power/ground. The application layouts have an average size of 1.54” x 0.80” for the TI TPS50601A-SP converters and 0.6” x 0.87” for a LTC3833 using GaN Systems GS61004B HEMTs. Bulk input and output capacitance on all boards utilize ceramic 47uF, 10V rated and 10uF, 50V rated X7R capacitors in 1210 packaging. All other capacitors used are automotive-grade 50V rated or higher with X7R dielectric.

Converter Test Setup

The converters were designed to operate with an input voltage of 5V and output voltages commonly used by modern processors of (1.0V, 1.8V, 3.3V) and corresponding currents (<6A). While the GaN and COTS converters are capable of operating at much higher output currents, the limitation was

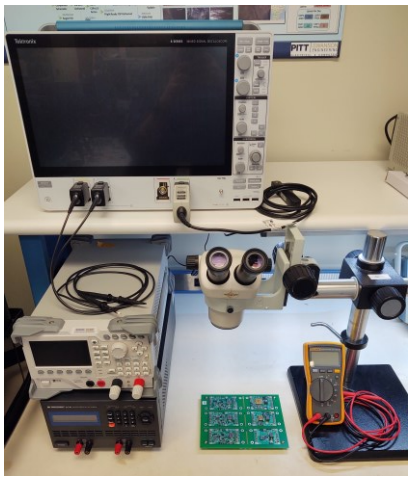

Figure 4. Test Equipment Setup for Converter Measurements

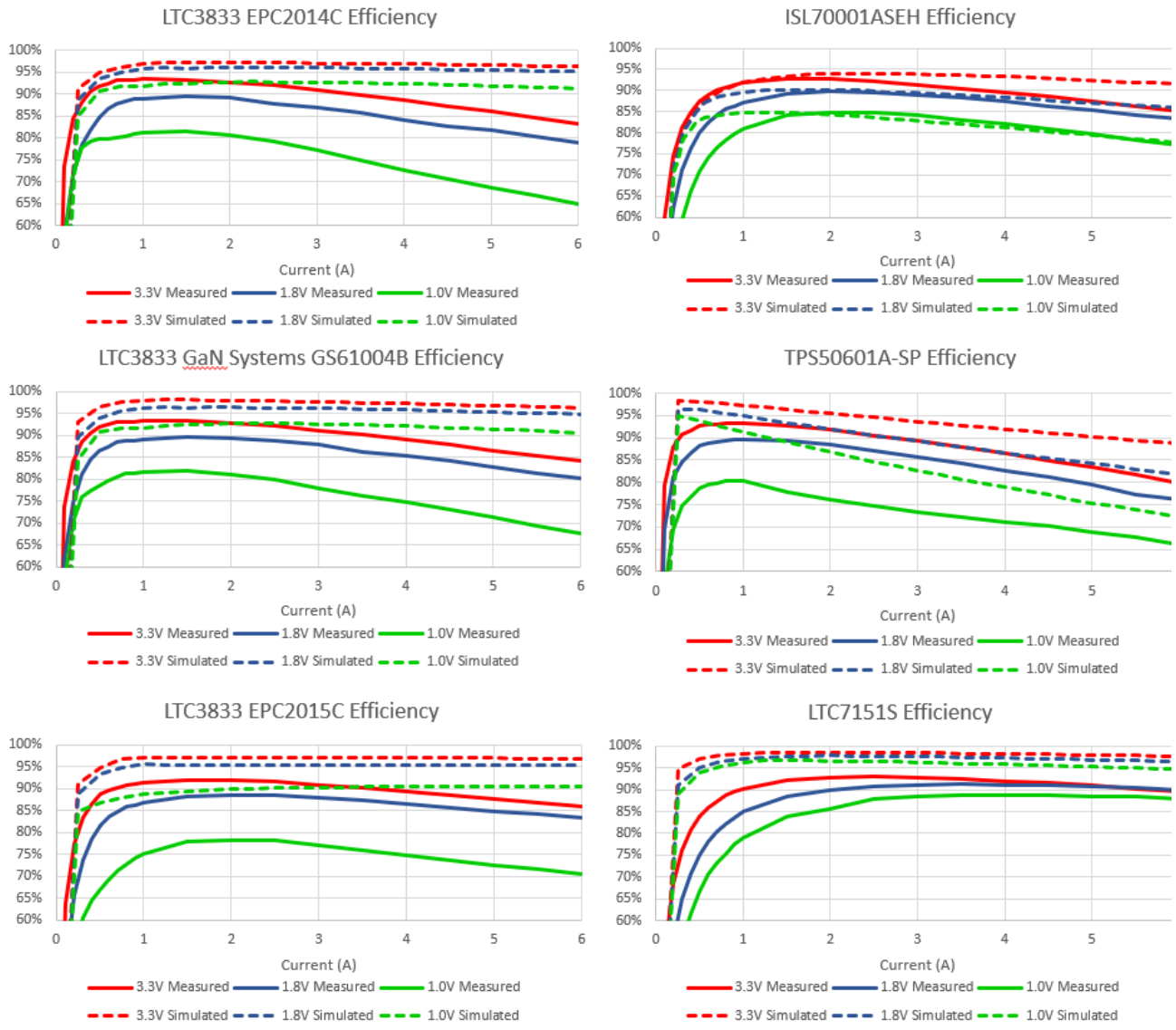

Figure 5. Simulated and Measured Efficiency of Converters

Table 3. Converter Output Characteristic Values

Parameters		Converters											
		TI TPS50601A-SP		Renesas ISL70001SEH		LT LTC7151S		LT LTC3833 with GaN Systems GS61004B HEMT		LT LTC3833 with EPC 2014c HEMT		LT LTC3833 with EPC 2015c HEMT	
		Simulated	*Measured*	*Simulated*	*Measured*	*Simulated*	*Measured*	*Simulated*	*Measured*	*Simulated*	*Measured*	*Simulated*	*Measured*
Output Voltage Ripple	*No Load*	0.4mV	1.557mV	N/A	1.748mV	0.2mV	3.156mV	1.51mV	1.055mV	0.4mV	1.332mV	0.4mV	1.610mV
	Full Load	0.3mV	3.369mV	N/A	2.068mV	0.2mv	3.742mV	0.9mV	2.516mV	0.2mV	1.482mV	0.2mV	1.557mV
Startup Transient (Voltage over nominal)	*1V*	10.21mV	0V	0V	0V	0.1mV	1.284mV	9.1mV	4.561mV	8.1mV	7.633mV	8.2mV	8.635mV
	1.8V	32.2mV	0V	0V	0V	0mV	4.947mV	6.5mV	3.028mV	5.2mV	18.934mV	5.1mV	3.454mV
	3.3V	80.3mV	0V	0V	0V	22mV	36.141mV	8.1mV	11.386mV	10.3mV	5.253mV	10.4mV	9.339mV
Load Change Transient (Voltage over nominal)	*1V*	83.6mV	79.104mV	70mV	66.567mV	30mV	20.149mV	37.6mV	18.550mV	36.9mV	18.017mV	35.8mV	17.484mV
	1.8V	90.7mV	47.335mV	70mV	33.475mV	32mV	22.281mV	54.3mV	28.145mV	53.8mV	29.744mV	53.3mV	27.079mV
	3.3V	131.7mV	84.686mV	68mV	37.207mV	66mV	30.810mV	170.5mV	43.070mV	58.2mV	44.883mV	57.4mV	36.674mV

imposed to simulate a CubeSat environment. All converters were simulated and measured for their turn ON and turn OFF transient behavior, load change transient response, full load and no-load output voltage ripple, switching waveforms, and efficiency. Thermal measurements were performed at an ambient temperature of 27°C from steady-state operation at a constant output current. Measurements were taken with a Tektronix MSO64 2.5GHz oscilloscope, Fluke 115 multimeter, Rigol DL3021 electronic load, BK-Precision 9183B DC power supply, and a FLIR E8 thermal imaging camera as shown in Figure 4.

6. Converter Results

The following section covers all of the simulated and measured results of the converters under test.

Converter Simulation Results

All converters were simulated using LTSpice and OrCAD prior to manufacturing. The SPICE models for the ISL70001ASEH converter were encrypted and therefore its simulations for output voltage ripple, and simulated efficiency were unable to be obtained so datasheet values were substituted. The SPICE model for the TPS50601A-SP converter had difficulty with output current values less than 100mA leading to an inaccurate efficiency plot as seen in Figure 5. For output current greater than 100mA the efficiencies were as expected. A simulated load step from 0 to 6A with a 1us rise and fall time was used. A selection of simulated waveforms is shown in Figure 6 with many of the waveforms being very similar across all converters under test.

Converter Hardware Results

Table 3 is a comparison summary of all the converter's output voltage ripples, voltage output transient responses to load stepping, and output voltage turn-on transients from both the simulated and measured converters. Output voltage ripple for both no-load and full load of all converters was higher than simulated which can be attributed to parasitic inductance and

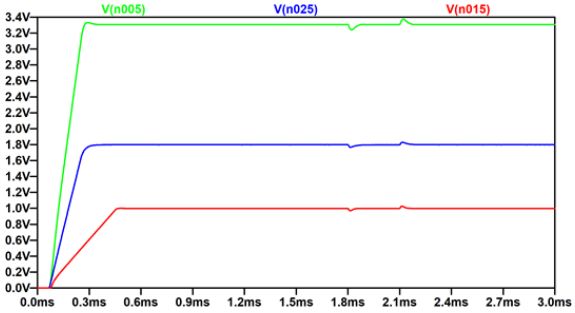

a) LT LTC7151S Load Step and Turn ON Output Voltage

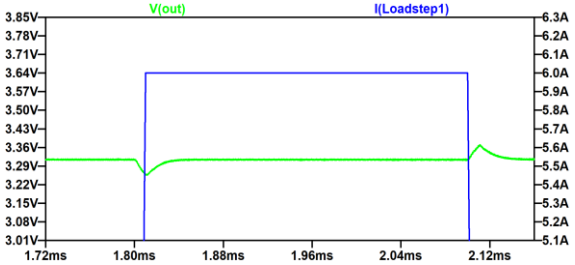

b) LTC3833 EPC2014C Load Step Transient

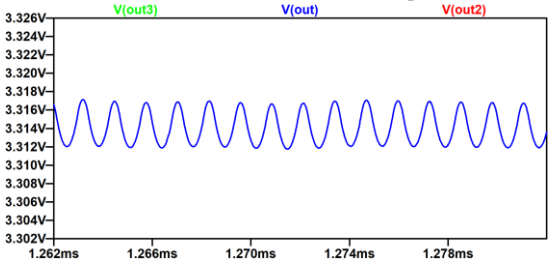

c) LTC3833 GaN Systems GS61004B Voltage Ripple

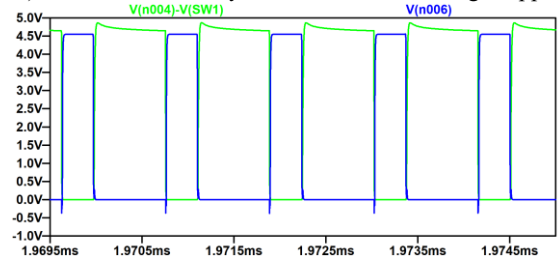

d) LTC3833 EPC2014C Gate Drive Signals

Figure 6. Simulated Waveforms of Converters

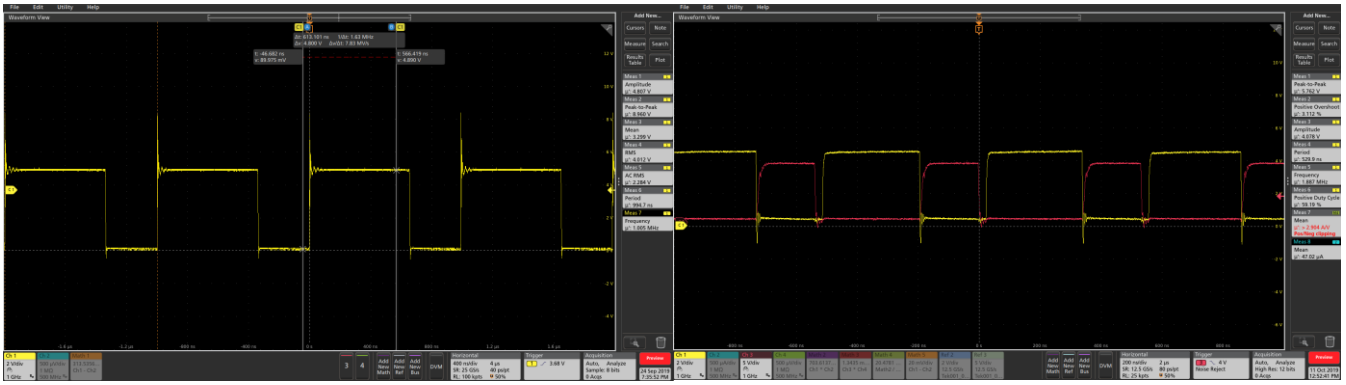

a) LTC3833 EPC2015C Switch Node Voltage. 400ns/div, 2V/div

b) Switching Waveforms LTC3833 EPC2014C. 400ns/div, 2V/div

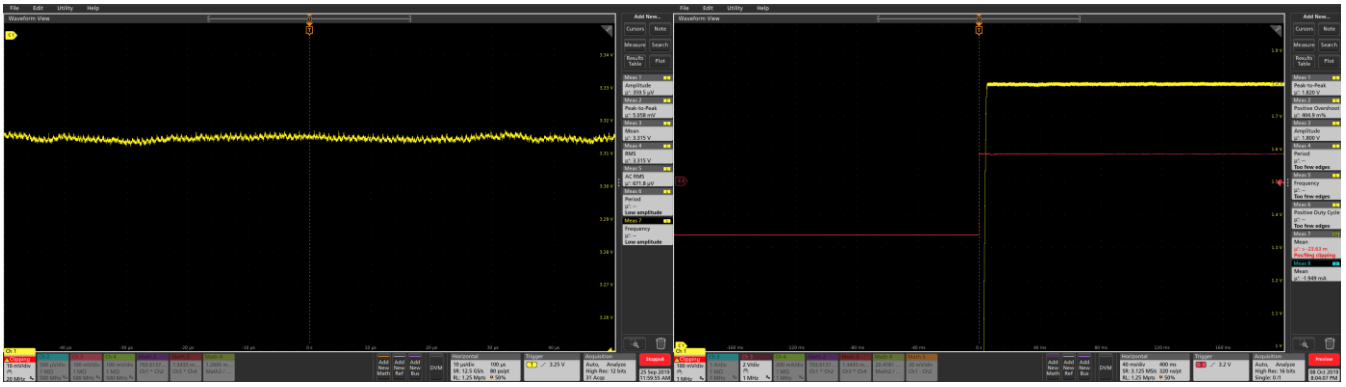

c) LTC3833 GaN Systems GS61004B Output Voltage Ripple. 10µs/div, 10mV/div

d) TPS50601A-SP Output Voltage Turn-On Transient (yellow), Input Voltage Turn-On (red). 40ms/div, 100mV/div

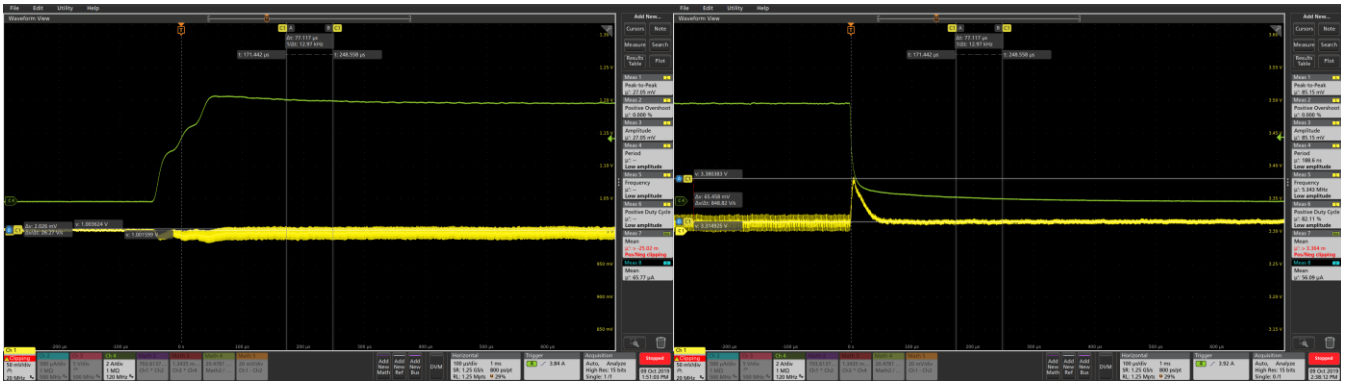

e) LTC3833 EPC2015C Load Turn ON Output Voltage Transient Response (yellow), Load Current (green). 10µs/div, 50mV/div

f) LTC3833 EPC2015 Load Turn OFF Output Voltage Transient Response (yellow), Load Current (green). 10µs/div, 50mV/div

Figure 7. Measured Waveforms of Converters

capacitance interaction with the switching waveforms. A selection of measured waveforms is shown in Figure 7. The simulated and measured efficiency plots for all converters at their respective output voltages of 1V, 1.8V, and 3.3V is shown in Figure 5. Efficiency measurements for all converters were below the simulation models due to parasitic losses in the PCB and components such as the inductor and capacitor equivalent series resistance.

The GaN converter's efficiency for 1.0V output was much lower than expected at the 6A output however, peak efficiencies above 80% were still seen for lower current values. This is attributed to switching loss at the GaN HEMTs and AC loss in the inductor. Improvements to efficiency can be made by reducing the parasitic inductance in the switch node and gate drive, thus reducing switching losses significantly. Overall output voltage ripple was at or below 2.5mV at full load which is well below the target of 20mV, as seen in Figure 7c. Generally, GaN converter turn ON and load change transients performed near or better than simulated with one significant outlier on the 1.8V GaN Systems based converter producing a turn-on voltage transient peak of 18.93mV. This transient was corrected by adjusting a resistor and capacitor in the compensation network.

The LTC7151S converter had consistently high efficiencies around 90%. LTC7151S measured output ripple was higher at both no load and full load conditions than the GaN and rad-hard converters at an average of 3.5mV. Startup transients were slightly higher than simulated by an average of 12mV with a max seen of 36.141mV for the 3.3V output which is above the desired 30mV transient specification. Load change transients were lower by an average of 20mV, all of which were at or under the 30mV transient specification.

The TPS50601A-SP efficiency had a peak above 90% for outputs of 3.3V and 1.8V and a peak of 80% for a 1.0V output. Output voltage ripple at full load was 3.369mV and 1.557mV at no load, well below the desired 20mV. Turn on voltage overshoot was 0V for all output voltages which was better than simulated. Output voltage transients during load change of the TPS50601A-SP were similar to the simulation for 1.0V and 3.3V outputs at 80mV, while the 1.8V output was much lower at 47mV. These values were above the desired 30mV transient specification.

The ISL70001ASEH had efficiencies all above 75% and results were similar to those listed in the datasheet since simulated values could not be generated. The startup transient response of the ISL70001ASEH had 0V overshoot exactly as simulated. During load change transient overshoot was seen to at or better than simulated by an average of 30mV for both 1.8V and 3.3V outputs, but still above the 30mV transient specification.

Thermal Results

The thermal performance of the converters showed that the GaN converters had most of their power loss and heat generation concentrated at the GaN HEMTs, which can be seen in the efficiency curves and attributed to switching loss. The thermal measurement results should prove for good reliability of the switching controller and the importance of a high thermal conductivity path for the GaN HEMTs when operating at high frequency. The switching losses led to the GaN converters being approximately 6ºC hotter than the rad-hard converters and 2ºC hotter than the COTs converter as shown in Figure 8. The GaN converters averaged 50ºC at full load, which is well below operating maximums of 105ºC. For the COTS and rad-hard converters, the heat is primarily generated at the converter, due to the nature of integrated MOSFETs. The vacuum of space this requires a more robust method of heat conduction on the board because convection cooling is not available in order to take heat away from the converter and improve its reliability. The packaging of the rad-hard converters has a high thermal conductivity and significantly attributed to keeping both devices to approximately 44ºC at full load. Both rad-hard converters operated well below their rated maximums of 125ºC and the LTC7151S operated at 49ºC, below its maximum of 125ºC.

7. DISCUSSION

The GaN converters had a better output voltage response than simulated with less output voltage ripple and less overshoot

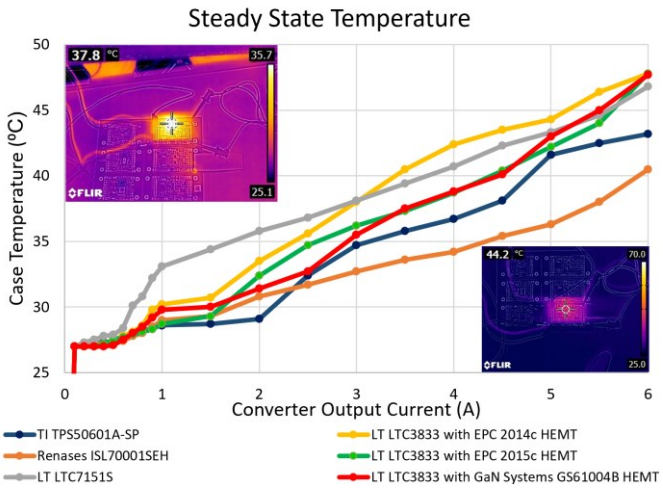

Figure 8. Steady-State Temperature at Output Current

than simulated. During load transients, the voltage dip and overshoot was less than simulated and indicates a high potential for usage in load-sensitive applications where very clean voltages are required. From testing, input and output capacitance can be reduced with minimal impact on performance, further saving space. The rad-hard converters performed similarly well, with very close output voltage characteristics, load change responses, and steady-state temperatures at a fixed output current. The advantage of the TPS50601A-SP is its reduced size and ability to sync with an additional TPS50601A-SP to output up to 12A. The LTC7151S had consistent transient responses for all output voltages and low output voltage ripple. The converter was very efficient over the full load range for all output voltages and was a power-dense solution. Overall, the GaN converters performed well when compared to the rad-hard and COTS equivalent converters.

COTS Controllers with External FETs

As processing systems and FPGAs increase in power, their core voltage drops and current increases beyond what most rad-hard converters can handle. For example, the Xilinx UltraScale+ XCVU13P core voltage V_{CCINT} supports 200A operating at 100ºC for 10 years [26]. The use of a COTS controller with a high current rated external FETs adds the ability to switch much higher currents than currently available integrated FET converters while still providing a power-dense solution.

Switched Converters as LDO Replacement

LDOs are inefficient when operating with a large voltage drop or a large output current since they primarily dissipate power through heat due to their linear nature. This makes them primarily suited for generating reference voltages. The benefit is an extremely clean output voltage with minimal noise and relative simplicity of integrating into a design. For MGTs, the efficiency tradeoff for clean voltage is severe, with efficiencies seen as low as 40% to 50% and high operational temperatures. The high switching frequency, fast

response time, and low output voltage ripple of the GaN converters allow them to react faster to load steps, minimizing the voltage overshoot and undershoot on powering sensitive high-speed transceivers. The high switching frequencies allow them to use smaller passive components like inductors and capacitors, further increasing power density and saving board space.

High Switching Frequency Impact

The higher switching frequencies capable from GaN means that the converter can respond faster to load step transients and puts less stress on the capacitors, requiring fewer of them, to maintain the same output voltage and eliminate droop. Due to fewer capacitors being required they become increasingly important to ensure that a clean voltage signal is coming through to the FPGA. Smaller value magnetics and capacitances have a greater effect on filtering the high frequencies; however, the source current draw from the PoL converter on the bus can potentially couple high-frequency noise into the ground plane causing previously unforeseen interactions with the FPGA.

Modular Power System Challenges

The modular converter power system offers several advantages for compute cards but also proposes some new challenges, namely mounting inductance, mechanical security, and thermal mitigation. By separating the power converter to a module, the electrical mounting pads ideally would be kept as short and wide as possible for decreased mounting inductance and increase structural and thermal contact. However, the large pad size requires a significant amount of board space taken up with unmasked copper, preventing any potentially necessary vias from being added into the board. The pad layout shown in Figure 1 was chosen to provide a 150mil by 250mil area for each pad with several vias to provide better electrical and thermal paths. Each pad's connection inductance is 1.16nH and its thermal impedance is 9.9ºC/W, with a total module thermal impedance of 2.5ºC/W. Inductance and thermal impedance were calculated using IPC standard equations based on via size, pad size, and number of pads. Since the converters are relatively lightweight with a low center of mass, mechanical stability is less of a concern with epoxy used for added mechanical strength.

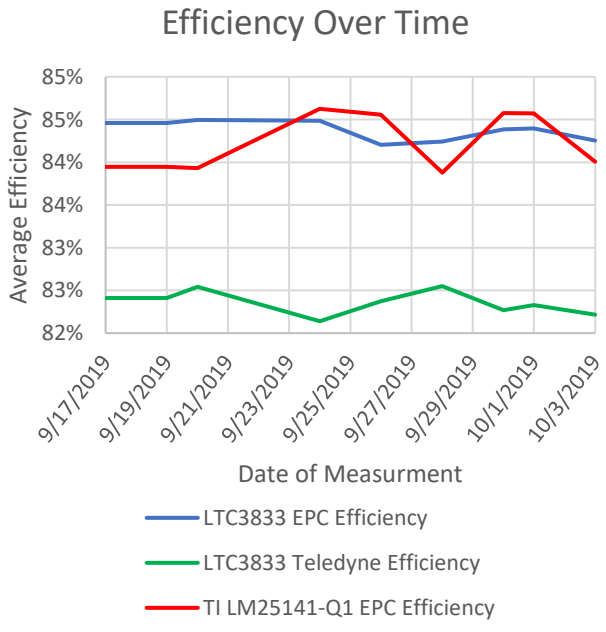

Figure 9. SSIVP GaN Converter Experiment Data

SSIVP GaN Converter Results

The GaN converters presented use technologies and components currently in orbit on the SSIVP experiment [3]. The SSIVP GaN sub-experiment is currently collecting voltage and current data to determine if total ionizing dose (TID) will cause drift in voltage regulation or efficiency capabilities or if recovery from a single event functional interrupt (SEFI) is recoverable. So far, preliminary data and initial passes through the South Atlantic Anomaly (SAA) have shown no effect on voltage regulation or efficiency as shown in Figure 9. Experimental data collection has been limited due to overall power limitations and priority of other additional experiments on SSIVP. Data is collected using a Texas Instruments (TI) INA260 and each converter is fused to prevent malfunctions from impacting the experiment. Sampling rate is limited so microsecond upsets where voltage goes out of regulation due to single event effects will likely not be captured.

8. Summary

The proposed GaN-based converters offer several advantages for scalability and power density when used for supplying FPGA systems. They offer clean, consistent output voltages over a wide load range and quick response times to load changes. The radiation tolerant nature of GaN, high switching frequency, and small size provides a significant cost reduction, size, and weight reduction for power systems while providing comparable efficiency to similar rad-hard components. The hybrid SSP currently utilizes the rad-hard TI TPS50601A-SP converters since they offer a power dense and efficient solution with excellent output voltage characteristics.

Acknowledgments

The research conducted in the paper was made possible in part by the industry and government members of the NSF SHREC Center and the IUCRC Program of the NSF under Grant No. CNS-1738783. The authors would like to thank Dr. Javier Valle at Texas Instruments for supplying the TI TPS50601A-SP converter and Paul Traynham at Renesas for providing the ISL70001ASEH converter for use in this research. We also thank Nicholas Franconi at NASA Goddard for his help with the PCB and converter design. Finally, we also thank the University of Pittsburgh Central Research Development Fund for providing the funding for building the converters and equipment acquisition.

REFERENCES

1. Lal, B., et al., *Global Trends in Small Satellites.* IDA Science and Technology Policy Institute, 2017: p. 401.
2. Doncaster, B., et al., *SpaceWorks' 2016 Nano/Microsatellite Market Forecast.* AIAA/USU Conference on Small Satellites, 2016. **30th Annual**: p. 6.
3. Cook, T., et al., *Radiation-Tolerant, GaN-based Point of Load Converters for Small Spacecraft Missions.* AIAA/USU Conference on Small Satellites, 2018. **32**(SSC18-XII-02): p. 1-10.
4. Petrick, D., et al. *SpaceCube v2.0 space flight hybrid reconfigurable data processing system*. in *2014 IEEE Aerospace Conference*. 2014.
5. Tsao, J.Y., et al., *Ultrawide-Bandgap Semiconductors: Research Opportunities and Challenges.* Advanced Electronic Materials, 2018. **4**(1).
6. Pearton, S., et al., *Ionizing radiation damage effects on GaN devices.* ECS Journal of Solid State Science and Technology, 2016. **5**(2): p. Q35-Q60.
7. Conversion, E.P., *EPC2014C.* Datasheet, 2019: p. 1-6.
8. Conversion, E.P., *EPC2015C.* Datasheet, 2019: p. 1-6.
9. Systems, G., *GS61004B.* Datasheet, 2018: p. 1-14.
10. Longobardi, G. *GaN for power devices: Benefits, applications, and normally-off technologies*. in *2017 International Semiconductor Conference (CAS)*. 2017.
11. Schwierz, F. *The frequency limits of field-effect transistors: MOSFET vs. HEMT*. in *2008 9th International Conference on Solid-State and Integrated-Circuit Technology*. 2008.
12. He, L., et al. *Evaluations and applications of GaN HEMTs for power electronics*. in *2016 IEEE 8th International Power Electronics and Motion Control Conference (IPEMC-ECCE Asia)*. 2016.
13. Systems, G., *Thermal Design for GaN Systems' Top-side cooled GaNpx-T Packaged Devices.* GN002 Application Note, 2018: p. 1-20.
14. Lidow, A. and R. Strittmatter. *Enhancement mode gallium nitride transistor reliability*. in *2015 IEEE First International Conference on DC Microgrids (ICDCM)*. 2015.
15. Jones, E.A., F.F. Wang, and D. Costinett, *Review of Commercial GaN Power Devices and GaN-Based Converter Design Challenges.* IEEE Journal of Emerging and Selected Topics in Power Electronics, 2016. **4**(3): p. 707-719.
16. Paula, W.J.d., et al. *A review on gallium nitride switching power devices and applications*. in *2017 Brazilian Power Electronics Conference (COBEP)*. 2017.
17. Bytkin, S.V. *Use of germanium doped silicon (n-Si<Ge>) for manufacturing radiation hardened devices and integrated circuits*. in *RADECS 97. Fourth European Conference on Radiation and its Effects on Components and Systems (Cat. No.97TH8294)*. 1997.
18. Hartwell, M., et al. *Total Ionizing Dose Testing of a RadHard-by-Design FET Driver in a 0.35µm Triple-Well Process*. in *2006 IEEE Radiation Effects Data Workshop*. 2006.
19. Gerardin, S., et al. *Radiation performance of new semiconductor power devices for the LHC experiment upgrades*. in *11th International Conference on Large Scale Applications and Radiation Hardness of Semiconductor Detectors*. 2015. SISSA Medialab.
20. Wang, J., et al., *Review of using gallium nitride for ionizing radiation detection.* 2015. **2**(3): p. 031102.
21. Scheick, L., *Single-Event Effect Report for EPC Series eGaN FETs: The Effect of Load Conditions on Destructive SEE.* Jet Propulsion Laboratory, National Aeronautics and Space Administration, 2014: p. 1-42.
22. Technologies, L., *LTC7151S.* Datasheet, 2018: p. 1-20.
23. Renesas, *ISL70001ASEH.* Datasheet, 2018: p. 1-26.
24. Instruments, T., *TPS50601A-SP.* Datasheet, 2018: p. 1-35.
25. Technologies, L., *LTC3833.* Datasheet, 2010: p. 1-36.
26. Xilinx, *UltraScale Architecture PCB Design User Guide.* Datasheet, 2019(UG583): p. 1-326.

BIOGRAPHY

Thomas Cook *received a B.S. in Engineering from the University of Pittsburgh in 2017. He is a graduate student researcher in the resilient and dependable computing group at the NSF Center for Space, High-performance, and Resilient Computing (SHREC) and at the Electric Power Systems Lab (EPSL) at the University of Pittsburgh. His research interests include wide-bandgap semiconductors, power electronics for space applications, and power systems for CubeSats.*

Aidan Phillips *received his B.S. degree in EE from The Pennsylvania State University and is a M.S. student and fellow at the NSF SHREC Center at the University of Pittsburgh. Aidan's research interest focus on power electronics, electromechanical systems, control theory, and radiation tolerant hardware for space applications.*

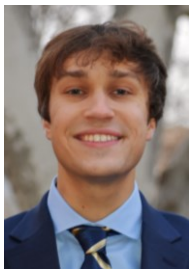

Christopher Siak *is a graduate student at the University of Pittsburgh, researching with the NSF Center for Space, High-Performance, and Resilient Computing (SHREC). His work with SHREC includes power efficiency analysis, power electronics system design, and software simulation development for small satellites.*

Dr. Alan D. George *(M'87-SM'93-F'13) is Department Chair and R&H Mickle Endowed Chair in Electrical and Computer Engineering in the Swanson School of Engineering at the University of Pittsburgh. He founded and directs the NSF Center for Space, High-performance, and Resilient Computing (SHREC), which replaced the NSF Center for High-performance Reconfigurable Computing (CHREC) in late 2017. Dr. George's research interests are in advanced architectures, apps, networks, services, systems, and missions for reconfigurable, parallel, distributed, and dependable computing. He is a Fellow of the IEEE.*

Dr. Brandon M. Grainger *is currently an assistant professor, Associate director of the Energy GRID Institute, and Associate director of the Electric Power Engineering Laboratory in the Department of Electrical and Computer Engineering at the University of Pittsburgh Swanson School of Engineering. Dr. Grainger's research interests are in electric power conversion, medium to high voltage power electronics, general power electronic converter design (topology, controller design, magnetics), resonant converters, high power density design, power semiconductor evaluation (SiC and GaN) and reliability assessment, military power systems, power electronic system interactions, fault identification techniques, and power electronics for aviation applications. In his career thus far, he has contributed to 60+ articles in the general area of electric power engineering (emphasis on electric power conversion) and all of which have been published through the IEEE, ASNE, or ASEE.*